Talanta ▮ (▮▮▮▮) ▮▮▮–▮▮▮

Contents lists available at SciVerse ScienceDirect

Talanta

journal homepage: www.elsevier.com/locate/talanta

Towards combinatorial spectroscopy: The case of minor milk fatty acids determination

I. Stefanov [a,*], V. Baeten [b], B. De Baets [c], V. Fievez [a]

[a] Laboratory for Animal Nutrition and Animal Product Quality (LANUPRO), Faculty of Bioscience Engineering, Ghent University, Proefhoevestraat 10, B-9090 Melle, Belgium
[b] Food and Feed Quality Unit, Valorisation of Agricultural Products Department, Walloon Agricultural Research Centre, Chaussée de Namur, 24. B-5030 Gembloux, Belgium
[c] Department of Mathematical Modeling, Statistics and Bioinformatics, Faculty of Bioscience Engineering, Ghent University, Coupure links 653, B-9000 Ghent, Belgium

ARTICLE INFO

Article history:
Received 1 October 2012
Received in revised form
13 February 2013
Accepted 17 February 2013

Keywords:
Trans MUFA
CLA
OBCFA
Combinatorial spectroscopy
ATR/FT-IR
Raman
Concatenation
Chemometrics

ABSTRACT

Chemometrical models for determination of milk fatty acids (FA) are typically developed using spectral data from a single spectroscopy technique, e.g., mid-infrared spectroscopy in milk control. Such models perform poorly in determining minor components and are highly dependent on the spectral data source and on the type of matrix. In milk fat, the unsuccessful determination of minor (fatty acids lower than 1.0 g/100 g in total fat) FA is often the result of: (1) the molecular structure similarity between the minor and the major FA within the milk fat matrix (thus the chemical signature specific to individual fatty acids has restricted specificity), and (2) the low signal intensity (detection limit) for specific vibrational modes. To overcome these limitations, data from different types of spectroscopy techniques, which brings additional chemical information in relation to the variation of the FA, could be included in the regression models to improve quantification. Here, Fourier transform (FT) Raman spectra were concatenated with attenuated total reflectance FT infrared (ATR/FTIR) spectra. The new combinatorial models showed up to 25% decrease in the root mean squared error of cross-validation (RMSECV) values, accompanied with a higher R^2_{cv} for most individual FA or sums of FA groups, as compared to regression models based on Raman only or ATR/FTIR only spectra. In addition, improved models included less PLS components indicating an increased robustness. Interpretation of the most contributing regression coefficients indicated the value of newly combined spectral regions as carriers of specific chemical information. Although requiring additional spectroscopy instrumentation and prolonged acquisition time, this new combinatorial approach can be automated and is sufficient for semi-routine determination of the milk FA profile.

1. Introduction

The animal production and food control fields are continuously evolving via advancements in analytical methodologies. Spectroscopy-based analytical techniques are particularly useful for disease and health condition screening and manufacturing process control, which when combined with accurate reference data and appropriate statistical methods can provide fast answers to the composition of various types of samples. The spectral bands not only depend on the types of chemical bonds, but are also correlated to their amounts present in the sample, which makes them very useful in quantification tasks [1]. Quantifications of fatty acids in different oil and food matrices via vibrational spectroscopy techniques have been intensely studied [2]. Knowledge of the fatty acids composition in milk is of importance to human health [3] and could provide useful information on the health status of dairy animals [4]. But milk has a complex fat matrix containing over 400 different fatty acids [5]. Due to their large number and structural variety, determination of milk fatty acids is considered a very difficult task not just by vibrational spectroscopy techniques, but also by conventional chromatography methods. Quantification of minor ($\leq$10 g/kg milk fat) milk fatty acids using vibrational spectroscopy becomes especially difficult in raw milk, due to the presence of other milk components, which interfere with fatty acid specific signals [6]. Minor fatty acid quantifications might also be difficult even when only the spectrum of milk fat is used for determinations [7]. In such cases, as well as when the constituent of interest is very minor ($<$0.5 g/100 g) and exhibits weak molecular vibration signals with hard to detect variations in concentration, new approaches

Abbreviations: ATR/FTIR, attenuated total reflectance Fourier transform infrared; CLA, conjugated linoleic acid; FA, fatty acid; GC, gas chromatography; IR, infrared; MIR, mid-infrared; MUFA, monounsaturated fatty acids; NIR, near-infrared; OBCFA, odd and branched chain fatty acids; PC, principal component; RMSECV, root-mean squared error of cross-validation; TFA, trans fatty acids; TLC, thin-layer chromatography

* Corresponding author. Tel.: +32 479196013; fax: +32 1 8605402525.
E-mail addresses: ivan@ivanstefanov.com, ivan_stefanov@yahoo.com (I. Stefanov).

0039-9140/$ - see front matter © 2013 Elsevier B.V. All rights reserved.
http://dx.doi.org/10.1016/j.talanta.2013.02.034

dealing with determinations of the milk fatty acid profile are required. One such novel approach would be to combine the spectrum of a milk fat sample from two different spectroscopy techniques and use the concatenated spectra for construction of better minor fatty acid determination models.

Infrared [IR, near-IR (NIR) and mid-IR (MIR)] and Raman spectroscopy are the main vibrational spectroscopy techniques proven useful in various routine and screening tasks, but there is a limit to the amount and the specificity of the information a particular technique provides [2]. The difference lies in the phenomenon behind each spectroscopy technique. IR represents a direct light absorption process and Raman spectroscopy is a light scattering process. In NIR, the absorbance bands are the overtones of the fundamental bands occurring in the MIR region. NIR bands are relatively weak, overlapped and are not clearly delineated. NIR is considered the least progressive of all vibrational spectroscopy techniques for the current task. In contrast, attenuated total reflectance Fourier transform mid-IR (ATR/FTIR) and Raman spectroscopy methods both measure the energy required to change fundamental vibrational and rotational energy states of chemical bonds. However, the absorption (ATR/FTIR) and scattering (Raman) phenomena have different rules governing their occurrence and thus offer differing sensitivities to the same functional groups, e.g. some vibrational transitions that are observed in IR spectroscopy are not observed in Raman spectroscopy. This results in different amounts of chemical information for the same compound by each technique, which makes the techniques complementary. Nevertheless, organic functional groups exhibit characteristic and well delineated bands when analyzed using ATR/FTIR and Raman spectroscopy. For example, the fatty acids' C=O carbonyl group is the most intensive MIR active absorption bands, whereas carbon double bonds C=C have strong isolated Raman scattering bands [8]. As a result of the sensitivity for various functional groups and the fundamental nature of the signal, Raman and ATR/FTIR can readily provide more useful analytical data as compared to NIR. All these features make Raman and ATR/FTIR ideal candidates in the new concatenation approach. Thus, here the spectra from both methods were combined for the first time in order to construct regression models for the determination of milk fatty acids.

2. Materials and methods

2.1. Sample selection

The sample storage and selection methodology was previously described [7]. Briefly, a total of 100 milk samples were selected from a sample bank ($n=1033$) of six different cow feeding experiments [7]. The sample subset was selected using a genetic algorithm applied to cover the naturally occurring concentration range of several milk fatty acids of interest, in particular odd and branched chain saturated fatty acids and several *trans*-C18:1 and *cis*/*trans*-C18:2 unsaturated isomers [9]. The milk fat was extracted using a previously described methodology involving dichloromethane–ethanol [10].

2.2. GC reference data

Quantification of *trans* fatty acids (TFA) and fatty acid groups using spectral data requires precise Gas Liquid Chromatography (GC) reference data for the construction of mathematical models. Identification and quantification of TFA through GC have been greatly improved with new highly polar, long capillary columns, but direct GC without prior fractionation could show overlapping between different *trans-n* and *cis-n* C18:1 positional isomers and *trans*-n C16:1 coelution with specific branched chain saturated and *cis-n* C16:1 mono-unsaturated FAs, which might result in an underestimation of the total TFA content [7,11]. Here, we used the temperature dependency of the polarity of cyanopropyl phases [12] to mathematically deduce concentrations of overlapping fatty acids using two different temperature programs without prior fractionation. A similar approach was described before [7,13,14]. After extraction, all samples were methylated [10] and fatty acid methyl esters (FAME) were analyzed by GC according to Vlaeminck et al. [15] (first temperature program) and by an isothermal ($T=180$ °C) (second) temperature program. Implementation of both temperature programs without prior separation on silver ion thin-layer chromatography (Ag^+ TLC), allowed quantification of individual *trans* monounsaturated FA, which coelute with branched chain saturated and specific *cis-n* monounsaturated FAs when only one GC temperature program is used. Due to a different separation with the second temperature program, most FA could be quantified individually as previously described [7,13]. As coelution of FA also depends on the column status, the identity of the FA and coeluting bands regularly requires confirmation by injections of Ag^+ TLC fractions. Due to a limited sample quantity for 8 of the 100 selected samples, GC profile reference data was available for 92 milk fat samples only.

2.3. Vibrational spectroscopy analysis

2.3.1. Fourier transform Raman spectroscopy

All Raman spectra were acquired on a Vertex 70—RAM II Bruker Fourier transform Raman spectrometer (Bruker Analytical, Madison, WI). The instrument is equipped with a Nd:YAG laser (yttrium aluminum garnet crystal doped with triply ionized neodymium) with an output at 1064 nm (9398.5 cm^{-1}). The maximum of the laser power is 1.5 W. The measurement accessory is pre-aligned, only the *Z*-axis of the backscattered light was adjusted to set the sample in the appropriate position regarding the local point and to maximize the scattering intensity. The 180° backscattering refractive geometry, CaF_2 beam splitter, and liquid nitrogen-cooled Ge diode array detector have been used. The OPUS 6.5 software for Windows of Bruker Instruments was used for the instrument management, spectral acquisition and file transformation. The spectral data were obtained with a resolution of 4 cm^{-1} and a nominal laser power of 600 mW. Milk fat samples and pure FA standards (~0.1–0.5 g/sample) were analyzed in vials selected by CRA-W in previous Fourier transform Raman analysis [8] with PE-caps (Klaus Ziemer GmbH, Mannheim, Germany), at room temperature (~25 °C) (RT) and immediately after freezing at −80 °C (FT). To ensure homogenization of the milk fat, all samples were melted at 38 ± 1 °C in a water bath, at a minimum of 1 h prior to temperature treatment. For each spectrum, 64 scans were co-added and averaged to obtain a good signal-to-noise ratio. A total of 3734 data points were recorded from 0 to 3599 cm^{-1}. Because of very low milk fat quantity in 14 and extraction solvent contamination in 3 of all 92 selected samples, Fourier transform Raman spectroscopy data in RT and FT were available for 75 milk fat samples.

2.4. ATR/FTIR spectroscopy

All attenuated total reflectance Fourier transform mid-infrared (ATR/FTIR) spectra were acquired on a Vertex 70RAM II Bruker spectrometer (Bruker Analytical, Madison, WI) operating with a Golden Gate ™ diamond ATR accessory (Specac Ltd., Slough, UK). The internal reflection element was a small, non-temperature-controlled Type IIa diamond prism allowing a sampled diameter of approximately 2.0 mm. The optically dense medium was in contact with two ZnSe focusing lenses, one used to focus the incident infrared radiation and the second one to collect the reflected infrared radiation. The optical bench included an interferometer with a RockSolid configuration, KBr substrate beam

Please cite this article as: I. Stefanov, et al., Talanta (2013), http://dx.doi.org/10.1016/j.talanta.2013.02.034

splitter and a deuterated triglycerin sulfate (RT-DLaTGS) detector. The OPUS 6.5 software for Windows of Bruker Instruments was used for instrument management, spectra acquisition and OPUS JCAMP to JCAMP-DX file transformation. The spectra were collected against air as a background over the wavenumber range of 4498–500 cm^{-1} with a resolution of 4 cm^{-1}. To ensure homogenization of the milk fat, all samples were melted in a 38 ± 1 °C water bath in vials selected by CRA-W in previous Fourier transform Raman analysis [16], at a minimum of 30 min prior to spectra acquisition. A small portion of each milk fat sample and FA standard (~0.1 g/sample) was placed on top of the optical medium and spectra were immediately acquired [room temperature (~24 ± 2 °C)], as well as selected FA standards were analyzed after freezing at −80 °C. For each spectrum, 64 scans were co-added and averaged to obtain a good signal-to-noise ratio. A total of 2074 data points were recorded from 4498-500 cm^{-1}. Because of very low milk fat quantity in 14 and extraction solvent contamination in 3 of all 92 selected samples, ATR/FTIR spectra were available for 75 milk fat samples. For each milk fat sample, ATR/FTIR and spectra were acquired in duplicate and the average of the two spectra was used for chemometrical analysis.

2.5. Data treatment

Data incorporation and standard partial least squares (PLS) regression were performed similarly to previous methodology [7]. A novel approach combining spectra from two different types of vibrational spectroscopy techniques was implemented by concatenation of the ATR/FTIR ($n=1241$) and Raman ($n=3734$) spectrum of each milk fat sample. However, the ATR/FTIR and Raman techniques are different in nature, thus each type of spectrum might require different pre-treatment, derivative transformation and variable (region) pre-selection methods:

- Multiplicative scatter correction (MSC) is considered adequate for Raman spectra pre-treatment and no difference between MSC or standard normal variate (SNV) was previously reported for ATR/FTIR spectra [17], thus MSC was the pre-treatment method of choice.
- ATR/FTIR based PLS models showed best results after derivative transformation on the full range spectrum [17].
- Raman spectra acquired at different temperature conditions [room temperature (RT) and after freezing the milk fat at −80 °C (FT)], as well as the combination of spectra of samples at both temperatures (RFT) showed opportunity for better predictions [7,8].
- Raman based PLS models included full spectra or manually selected regions (1650 variables) that are commonly believed to be the chemical information carriers (3100–2600 and 1850–750 cm^{-1}) [16].

Thus, in order to examine the performance of the different models, all possible combinations of the ATR/FTIR spectra without derivative transformation, after 1st Savitzky–Golay (SG) derivative or after 2nd SG derivative transformation with RT, FT and RFT Raman milk fat spectra (Scheme 1) were subjected to a backward variable elimination procedure (Scheme 2) using the "jackknifing" variable selection method with PLS (NIPALS algorithm) in The Unscrambler™ software (CAMO, Trondheim, Norway). This backward variable elimination approach resulted in 18 different PLS models for each individual fatty acid (FA) and FA groups [mono-unsaturated *trans* fatty acids (MUFA): *trans*-4 C18:1, *trans*-5 C18:1, *trans*-6+7+8 C18:1, *trans*-9 C18:1, *trans*-10 C18:1, *trans*-11 C18:1, *trans*-12 C18:1, *trans*-15 C18:1 and total low, mid and high *trans* MUFA; conjugated linoleic acids (CLA): *cis*-9, *trans*-11 C18:2 and *trans*-10, *cis*-12 C18:2; total CLA; odd and branched chain saturated fatty acids (OBCFA): *iso* C13:0, *ante* C13:0, *iso* C14:0, *iso* C15:0, *ante* C15:0, C15:0, *iso* C16:0, *iso* C17:0, *ante* C17:0 and C17:0, total ODD (sum of C5:0, C7:0, C9:0, C11:0, C15:0, C17:0, C19:0, C21:0, C23:0), total ISO (sum of *iso* C13:0, *iso* C14:0, *iso* C15:0, *iso* C16:0, *iso* C17:0 and *iso* C18:0), total ANTE (sum of *ante* C13:0, *ante* C15:0 and *ante* C17:0), total BRANCHED (sum of ISO and ANTE) and total OBCFA (sum of ODD and BRANCHED)].

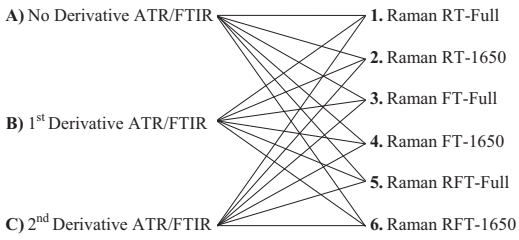

Scheme 1. Combinatorial models for concatenation of attenuated total reflectance Fourier transform mid-infrared (ATR-FTIR) and Raman spectra obtained at room temperature (RT), after freezing at −80 °C (FT) and a combined RT and FT (RFT) of milk fat using a backward variable elimination approach as indicated in Scheme 2.

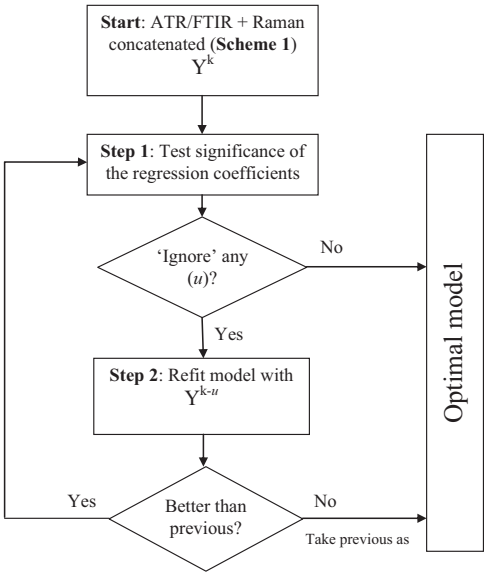

Scheme 2. Backward variable elimination strategy.

However, the extraction of an optimal set of wavenumbers specific to fatty acids using this backward variable elimination procedure (used to select variables that correlate with the measured parameter and to reject data from absorbance and scattering bands not contributing to the prediction) might be obscured from the high dimensionality of the so combined ATR/FTIR and Raman spectra. For this, a forward [pre-selecting the best Raman only predictors (based on previous PLS models using Raman spectra only [7,8]) and then combining them with the ATR/FTIR spectrum] variable selection methodology was evaluated (Scheme 3). The so pre-selected Raman bands were combined with either:

- the full ($n=1241$) ATR/FTIR spectra (Scheme 3A);
- manually selected ATR/FTIR regions, which are commonly believed to be the most important signal carriers [18] (Scheme 3B);

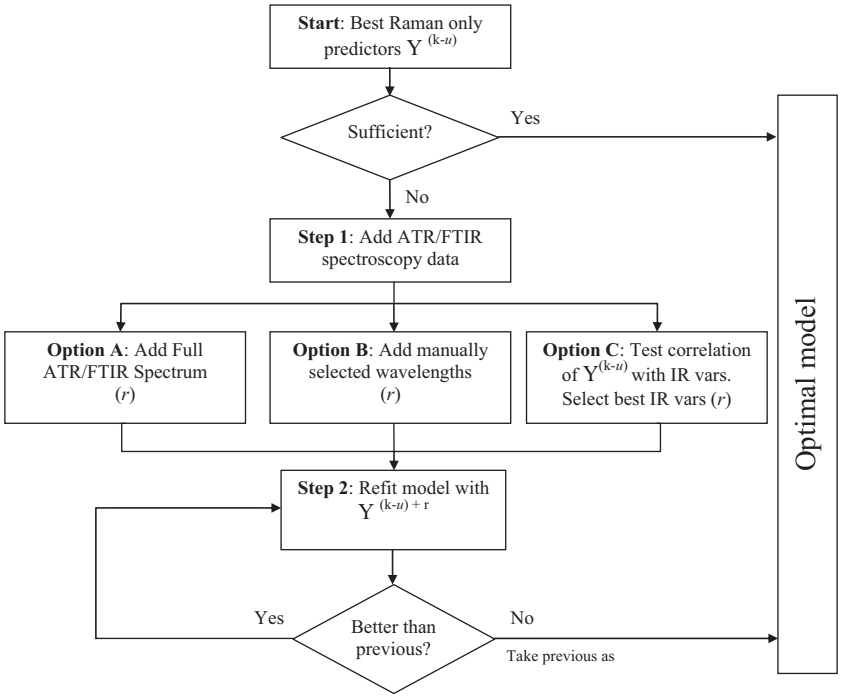

Scheme 3. Forward variable selection strategy.

- variables from the ATR/FTIR spectra, which had greater than $R^2 > 0.50$ cross-correlation with the best Raman only pre-selected predictors (Scheme 3C).

This forward variable selection approach was expected to preserve the most useful spectral information and lower the complexity of the data matrix, which should result in simpler and more robust FA prediction models. The former resulted in three additional regression models (for a total of 21 PLS models) for each individual and grouped FA of interest. For all PLS models validation was carried out using systematic cross-validation with 3 folds and 25 units per segment. The optimal number of PLS factors used for the regression was determined from the minimum residual validation variance.

3. Results

3.1. PLS regression

3.1.1. Variable selection

The new combinatorial models based on backward variable elimination (Scheme 2) showed an improved or similar performance for at least one combination of attenuated total reflectance Fourier transform mid-infrared (ATR/FTIR) spectra (without derivative, 1st or 2nd Savitzky–Golay derivative) and Raman (RT, FT or combined RFT) spectra, compared to models with individual ATR/FTIR only or individual Raman only spectra. The combinatorial results presented in Tables 2 and 3 show the fatty acid (FA) models with the highest cross-validation coefficient of determination (R^2_{cv}) and the lowest root mean squared error of cross-validation (RMSECV) parameters. The percent improvements over previously reported results for individual ATR/FTIR only and Raman only spectra models are presented in Figs. 1 and 3 and Figs. 2 and 4, respectively.

In contrast, the forward variable selection approach (Scheme 3) most models for prediction of individual and grouped FA (results not shown), with an average between 10% and 40% lower performance (based on lower R2cv and higher RMSECV) compared to single spectra models.

3.2. Saturated OBCFA

The best combinatorial models for both individual odd chain fatty acids C15:0 and C17:0 were somewhat improved over the optimal single Raman models (Fig. 3) and drastically better than the best single ATR/FTIR models (Fig. 1). While C15:0 and all other fatty acid improvements were achieved using a backward variable selection strategy, the C17:0 was the only FA determined better when a forward variable selection method was used.

Not surprisingly, the total saturated odd chain fatty acid group (ODD) was influenced by the individual FA improvements and the optimal ODD group model had more than 11% decrease in RMSECV compared to Raman only (Fig. 3). Similarly, the OBCFA model was also influenced by the C15:0 presence (Supporting materials, Fig. SM1) and variables in the vicinity of 1302 cm^{-1} (ATR/FTIR) and 1040 cm^{-1} (Raman) also occurred as significant regression coefficients in the best OBCFA combinatorial model.

3.3. ISO

All *iso* branched chain FA combinatorial models, except for *iso* C15:0, had improved R^2_{cv} and RMSECV parameters (Figs. 1 and 2). But while the *iso* C13:0 and *iso* C17:0 models promised sufficient for semi-routine determinations, the performance of the best *iso* C14:0 and *iso* C16:0 combinatorial models remained poor. The best *iso* C17:0 combinatorial model resulted in 20% increase in R^2_{cv}, reaching 0.80 with a 25% lower RMSECV (0.025) and only four PCs (Table 2, Fig. 2).

Combinatorial models for one of the least abundant branched chain fatty acids *iso* C13:0 (very minor concentration of less than 0.1 g/100g) obtained the largest gain compared to all other OBCFA. This was the result of combined signals from the ATR/FTIR and RFT Raman spectra, which were similar compared to the previously reported *iso* specific signals [7], but slightly shifted (Supporting materials, Fig. SM2). In addition, other bands from

Table 1
Concentration range of individual and grouped *trans* monounsaturated (*trans* MUFA), conjugated linoleic (CLA) and odd and branched chain (OBCFA) fatty acids in milk fat (g/100 g of FAME, $n=75$).

Fatty acid	Min	Max	Average	Std. Dev.
C18:1*trans*-4	0.006	0.074	0.020	0.010
C18:1*trans*-5	0.006	0.108	0.018	0.015
C18:1*trans*-6+7+8	0.105	1.079	0.254	0.157
C18:1*trans*-9	0.113	1.155	0.232	0.181
C18:1*trans*-10	0.113	11.74	0.945	2.320
C18:1*trans*-11	0.170	4.925	0.950	0.908
C18:1*trans*-12	0.125	1.424	0.316	0.220
C18:1*trans*-15	0.023	0.515	0.152	0.103
***trans*MUFA**[a]	1.475	21.01	4.538	4.168
C18:2*cis*-9, *trans*-11	0.005	1.958	0.437	0.405
C18:2*trans*-10, *cis*-12	0.000	0.038	0.013	0.008
CLA[b]	0.056	2.041	0.472	0.446
C15:0	0.462	2.590	1.440	0.345
C17:0	0.301	0.777	0.434	0.101
ODD[c]	1.110	4.430	1.840	0.548
***iso* C13:0**[d]	0.012	0.048	0.029	0.008
***iso* C14:0**[d]	0.033	0.115	0.068	0.019
***iso* C15:0**[d]	0.116	0.283	0.187	0.027
***iso* C17:0**[c]	0.155	0.467	0.265	0.054
ISO[d]	0.572	1.100	0.766	0.100
ante C15:0	0.167	0.533	0.406	0.070
ante C17:0	0.288	0.520	0.357	0.063
ANTE[e]	0.533	1.050	0.775	0.115
BRANCHED[de]	1.230	2.030	1.540	0.181
OBCFA[cde]	2.341	5.940	3.380	0.597

[a] Individual FA reported as well as all *trans* C14:1 and all *trans* C16:1 are included in the sum of trans monounsaturated fatty acids (*trans* MUFA).
[b] Individual FA reported as well as *trans*-9, *cis*-11 C18:2 and *trans*-11,*cis*-13+*cis*-9, *cis*-11 C18:2 are included in the sum of conjugated linoleic acids (CLA).
[c] Individual FA reported as well as C5:0, C7:0, C9:0, C11:0, C13:0, C19:0, C21:0, C23:0 are included in the sum of Odd Chain Fatty Acids (ODD).
[d] Individual *iso* FA reported as well as *iso* C16:0 and *iso* C18:0 are included in the sum of *iso* branched chain fatty acids (ISO).
[e] Individual *anteiso* FA reported are included in the sum of *anteiso* Branched Chain Fatty Acids (ANTE).

Table 2
Partial least squares regression results for the best individual and grouped saturated odd and branched (*iso* and *ante*) chain fatty acids (OBCFA) using no derivative, 1st Savitzky–Golay (SG) or 2nd SG derivative transformation *for ATR/FTIR spectra combined with RT, FT or RFT Raman spectra of milk fat samples ($n=75$) after multiplicative scatter correction (MSC) transformation. Best results (bold) are based on lower RMSECV[a], lower no. PCs and higher R^2_{cv} compared to ATR/FTIR only or Raman only spectra models.

	Combinatorial spectroscopy models						Single spectroscopy models		
				ATR/FTIR	Raman		ATR/FTIR	Raman	
Fatty acid	R^2_{cv}	RMSECV	No. PCs	SG*	*T* (°C)[b]	Range	SG	*T* (°C)[b]	Range
C15:0	**0.728**	**0.179**	**4**	No Der	RFT	Full	1st	FT	Full
C17:0	0.553	0.071	7	1st	RT	Full	2nd	RT	Full
ODD	**0.688**	**0.312**	**4**	2nd	FT	Full	1st	RFT	Full
***iso* C13:0**	**0.632**	**0.005**	6	1st	RFT	Full	No Der	RFT	Full
***iso* C14:0**	**0.377**	**0.015**	**3**	1st	FT	Full	2nd	FT	1650
***iso* C15:0**	0.514	0.019	4	1st	RFT	Full	No Der	RFT	Full
***iso* C16:0**	**0.373**	**0.034**	**4**	1st	FT	Full	1st	FT	Full
***iso* C17:0**	**0.799**	**0.025**	**4**	1st	FT	Full	No Der	FT	Full
ISO	0.367	**0.079**	4	2nd	FT	Full	2nd	FT	Full
***ante* C13:0**	**0.466**	**0.003**	**4**	2nd	FT	Full	1st	FT	Full
***ante* C15:0**	**0.749**	**0.035**	7	2nd	RFT	1650	2nd	RFT	Full
***ante* C17:0**	0.793	0.029	6	2nd	RFT	Full	2nd	RFT	Full
ANTE	0.809	0.051	7	1st	RFT	Full	2nd	RFT	Full
BRANCHED	**0.719**	**0.096**	7	2nd	RFT	Full	1st	RFT	Full
OBCFA	**0.771**	**0.284**	**2**	2nd	FT	1650	2nd	FT	Full

[a] Root mean square error of cross-validation (RMSECV) in g/100 g fatty acid methyl esters (FAME).
[b] Raman spectra of milk fat samples acquired at room temperature (RT), after freezing at −80 °C (FT) or combined RT and FT (RFT).

the Raman spectra in the vicinity of 2074 cm^{-1} appeared as significant (Supporting materials, Fig. SM2). However, the former are rather noisy and are not related to any scattering signals, thus their appearance could only be attributed to a variation shift from other important bands (such as the C=O band in the vicinity of 1700–1780 cm^{-1}) to noise containing regions during the multiplicative scatter correction (MSC) pre-processing technique [19] (Supporting materials, Fig. SM3). Nevertheless, it was interesting to observe that these same bands appeared as significant in both the RT Raman and the FT Raman parts of the *iso* C13:0 model (Supporting materials, Fig. SM2).

3.4. ANTE

No drastic improvement for the individual and grouped ANTE fatty acids was evident, with the exception of a slight numerical increase in R^2_{cv} and RMSECV for *ante* C13:0 and *ante* C15:0 (Table 2, Fig. 2). Already the best *ante* C17:0 models based on single Raman spectra had satisfactory performance, but no additional useful combinatorial information related to the variation of this FA within this concentration range using the current dataset was available. Similarly to *iso* C17:0, the regression coefficients plot of the best *ante* C17:0 model indicated significant predictors in the vicinity of 3060–3020 cm^{-1} and 3015–3005 cm^{-1} (Supporting materials, Fig. SM4), which was in support for the assumption for saturation information presence in this part of the Raman spectrum (Fig. 5).

3.5. Unsaturated FA

In general, the combinatorial models for the *trans*-mono and *trans*-conjugated unsaturated FA resulted in lesser improvement when compared to the saturated OBCFA gain over single spectra models. This might be a consequence of the already good determinations with the single Raman or ATR/FTIR spectra models, which contain directly available isolated non-overlapping chemical signals specific to *trans*-mono and *trans*-conjugated unsaturated bonds [8]. Nevertheless predictions of some of the minor fatty acids were improved, while for others although no improvement in the models' RMSECV or R^2_{cv} parameters occurred, a decrease in the number of model factors was evident (Table 3).

3.5.1. Trans MUFA

The best combinatorial *trans*-6+7+8 C18:1 FA model had no improvement in R^2_{cv} and RMSECV over individual spectra results, but the number of principal components (PCs) used for description of the variation significantly decreased (4 PCs compared to 6 PCs for single Raman). The *trans*-6+7+8 C18:1 regression coefficients were similar to previously reported bands in the Raman spectra [8], but the new model required only 55 predictor variables from the concatenated Raman+ATR/FTIR spectra

Table 3
Partial least squares regression results for the best individual and grouped *trans* monounsaturated (*trans* MUFA) and conjugated linoleic (CLA) fatty acids using no derivative, 1st Savitzky–Golay (SG) or 2nd SG derivative transformation* for ATR/FTIR spectra combined with RT, FT or RFT Raman spectra of milk fat samples after multiplicative scatter correction (MSC) transformation. Best results (bold) are based on lower RMSECV[a], lower No PCs and higher R^2_{cv} compared to ATR/FTIR only or Raman only models.

Fatty acid	*n*	g/100 g	Combinatorial spectroscopy models						Single spectra models		
			R^2_{cv}	RMSECV	No. PCs	ATR/FTIR	Raman		ATR/FTIR	Raman	
						SG*	T (°C)[c]	Range	SG	T (°C)[c]	Range
C18:1 *trans*-4	75	Max[b]	**0.778**	**0.005**	7	No Der	FT	Full	2nd	FT	Full
C18:1*trans*-5	75	Max[b]	**0.659**	**0.009**	**4**	1st	RFT	Full	No Der	RFT	1650
C18:1 *trans*-6+7+8low	73	< 0.50	0.855	0.031	**4**	1st	FT	Full	2nd	RFT	Full
C18:1 *trans*-6+7+8	75	Max[b]	**0.402**	**0.122**	**3**	2nd	FT	1650	No Der	FT	1650
C18:1 *trans*-9 low	70	< 0.42	0.902	0.020	5	2nd	RFT	Full	1st	RFT	Full
C18:1 trans-9 low	75	Max[b]	**0.945**	**0.047**	5	2nd	FT	Full	1st	FT	1650
C18:1 *trans*-10 low	68	< 0.84	0.753	0.076	5	2nd	RFT	1650	2nd	FT	Full
C18:1 *trans*-10	75	Max[b]	**0.946**	**0.543**	**5**	1st	RFT	1650	1st	RFT	1650
C18:1 *trans*-11 low	66	< 1.20	0.781	0.100	5	2nd	FT	Full	No Der	RT	1650
C18:1 *trans*-11	75	Max[b]	0.926	0.245	**1**	No Der	FT	Full	No Der	RT	1650
C18:1 *trans*-12 low	73	< 0.91	**0.876**	**0.054**	4	2nd	FT	1650	2nd	FT	1650
C18:1 *trans*-12	75	Max[b]	**0.814**	**0.094**	6	No Der	RT	1650	1st	RFT	1650
C18:1 *trans*-15	75	Max[b]	**0.737**	**0.052**	**5**	2nd	FT	Full	2nd	FT	Full
***trans* MUFA low**	63	< 4.60	**0.901**	**0.195**	5	No Der	RT	Full	2nd	FT	Full
***trans* MUFA mid**	70	< 8.10	**0.962**	**0.213**	6	1st	RFT	Full	2nd	RFT	Full
***trans* MUFA high**	75	Max[b]	0.987	0.474	7	2nd	RT	1650	1st	RT	1650
C18:2 *cis*-9, *trans*-11	75	Max[b]	0.860	0.142	**4**	1st	RT	Full	1st	RFT	1650
C18:2 *trans*-10, *cis*-12	75	Max[b]	0.729	0.004	**4**	2nd	FT	Full	2nd	FT	Full
CLA	75	Max[b]	0.942	0.098	**3**	2nd	RT	Full	1st	RT	Full

[a] Root mean square error of cross-validation (RMSECV) in g/100 g fatty acid methyl esters (FAME).
[b] Maximum concentration in g/100 g FAME of the corresponding fatty acid (FA) or FA group as reported in Table 1.
[c] Raman spectra of milk fat samples acquired at room temperature (RT), after freezing at −80 °C (FT) or combined RT and FT (RFT).

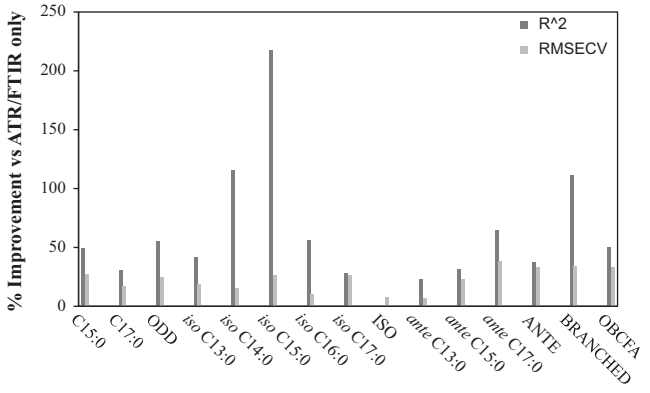

Fig. 1. Percent increase in performance of R^2_{cv} and RMSECV for the best (as indicated in Table 2) individual and grouped odd and branched chain saturated fatty acid combinatorial models compared to the best individual ATR/FTIR only spectra models.

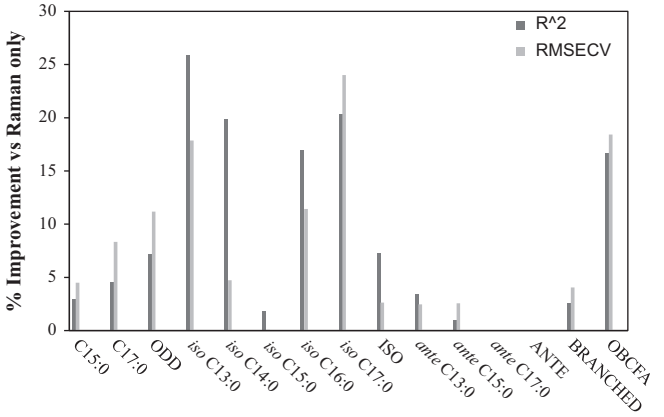

Fig. 2. Percent increase in performance of R^2_{cv} and RMSECV for the best (as indicated in Table 2) individual and grouped odd and branched chain saturated fatty acid combinatorial models compared to the best individual Raman only spectra models.

(compared to 72 for the best Raman only, Supporting materials, Fig. SM5).

The optimal total *trans* MUFA in low concentration range (< 4.6 g/100g in total fat) combinatorial model showed fine improvement over single Raman and ATR/FTIR. Although, the presence of conjugated linoleic acids (CLA) is known to hinder *trans* MUFA determinations in low quantities with ATR/FTIR analyses (AOCS Official Method Cd 14d-99) due to proximity of conjugated and isolated *trans* unsaturated FA signals in the vicinity of 930–990 cm^{-1} [17], the newly resulted interaction with the Raman part of the spectra in the vicinity of 1670 cm^{-1} overcame this difficulty (Supporting materials, Fig. SM6). The 1666 cm^{-1} Raman scattering was previously reported as *trans* MUFA specific [8]. This indicates an opportunity for routine screening of low *trans* MUFA.

3.6. CLA

Although the R2cv and RMSECV parameters for any individual or grouped CLA combinatorial models remained unimproved, the simplicity of the new models was evident by the lower number of factors required for description of the FA variation. The best models for the two individual *trans*-10, *cis*-12 and *cis*-9, *trans*-11 CLA isomers required four principal components (compared to 7 PCs for single Raman and 7 PCs for single ATR/FTIR) and the total CLA group model had only three PCs (compared to 7 PCs for single Raman and 5 PCs for single ATR/FTIR, Table 3). This improvement in simplicity was supported by the lower number of significant predictors: 62 predictor variables for the total CLA group and only 21 for the *cis*-9, *trans*-11 CLA isomer. Based on the regression coefficients plot of the latter, the explained variation

emerged from the Raman spectrum in the vicinity of 1652 cm^{-1} and the ATR/FTIR spectrum in the vicinity of 945 cm^{-1}, which is consistent with previously reported bands [8].

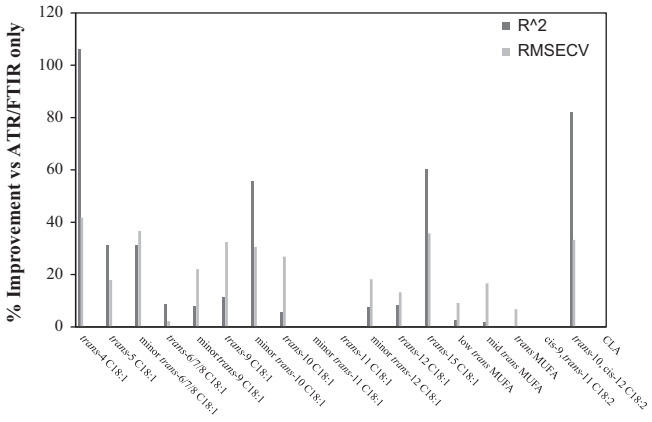

Fig. 3. Percent increase in performance of R^2_{cv} and RMSECV for the best (as indicated in Table 2) individual and grouped *trans*-mono and conjugated unsaturated fatty acid combinatorial models compared to the best individual ATR/FTIR only spectra.

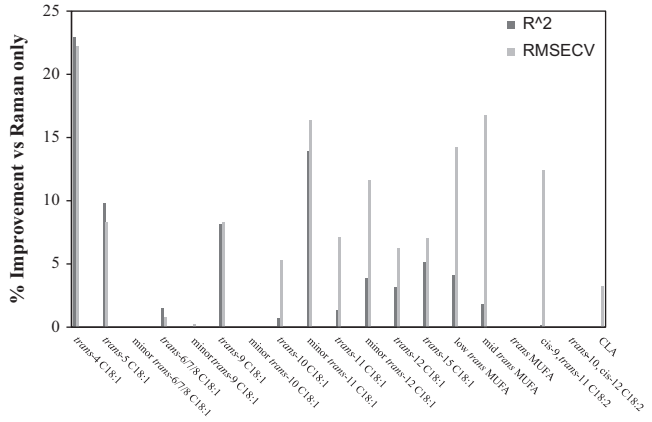

Fig. 4. Percent increase in performance of R^2_{cv} and RMSECV for the best (as indicated in Table 2) individual and grouped *trans*-mono and conjugated unsaturated fatty acid combinatorial models compared to the best individual Raman only spectra models.

4. Discussion

Improvement of milk fatty acid quantification models is currently performed by (1) extending the calibration range (increasing in dependent variation in the response variable), or (2) increasing the number of spectra used in the calibration model [6], or both. Although the first approach could increase the strength of the relationship between the predictors and the response variable, it improves model performance by increasing linearity, but does not necessarily decrease the residuals for lower range predictions. Further, the second approach might increase precision by minimizing perturbation from other non-targeted constituents (such as protein, lactose, urea and water), but it does not necessarily improve the accuracy of the predictions by adding new vibrational information specific to fatty acids. The latter cannot help with quantification models for minor constituents such as minor fatty acids (below 1.0 g/100g of total fat), which exhibit little or no detectable variations in absorption/scattering signal specific to their molecular structure. Thus, to achieve actual improvement in accuracy there is a need to (1) remove the perturbation of non-targeted milk constituents and/or (2) add more vibrational information (predictors) specific to the minor fatty acids of interest. The former was already implemented by extracting the milk fat and using spectra of the milk fat only for construction of calibration models. The latter could be achieved by analyzing the sample of interest under different environmental conditions (varying temperature etc.) and was already accomplished using Raman spectroscopy [7,8]. However, if the spectral information from one technique is not capable in providing a sufficient answer to a specific question, often additional techniques are used for providing this extra vibrational information, e.g. application of more than one spectroscopy technique as a secondary confirmation for the identity of chemicals is an established procedure in the pharmaceutical, forensic and many other fields [20–22]. Similarly in the food control and animal production field, if a chemical of interest is difficult to analyze (due to similarities in the chemical structures with other components and/or low amounts in the matrix), but exhibits a characteristic chemical signal with more than one spectroscopy technique, it would be useful to utilize the information from the various spectra. Because the Raman spectrum of milk fat is complementary to the mid-infrared (IR) spectrum that may be obtained for the same sample (that is, both techniques possess characteristic signals for specific fatty acid chemical bonds, but with different intensities and band positions), their combination for prediction of individual or grouped fatty acids (FA) is compelling.

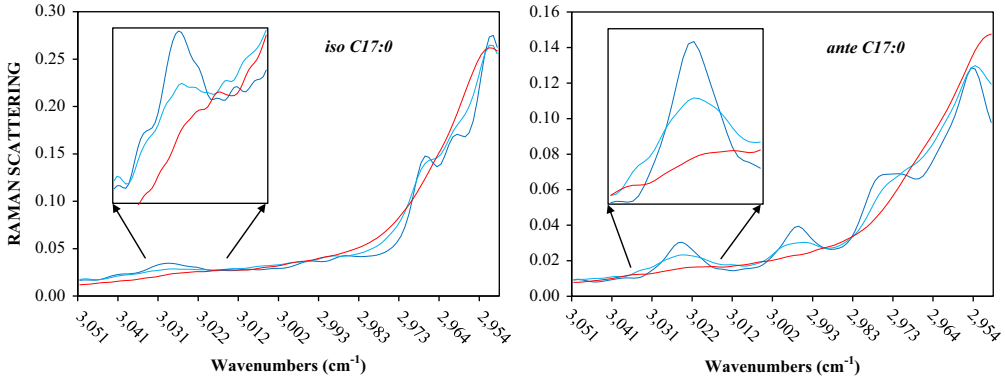

Fig. 5. Multiplicative scatter corrected (MSC) Raman spectra of *iso* C17:0 and *ante* C17:0 branched chain saturated fatty acid methyl ester standards acquired at room temperature (red line, RT), after freezing at −80 °C (baby blue, FT) and after freezing with liquid nitrogen (dark blue, LN) in the 3050–2950 cm^{-1} region. (*x*-axis: wavenumbers (cm^{-1}), *y*-axis: scattering units). (For interpretation of the references to color in this figure legend, the reader is referred to the web version of this article.)

4.1. Simplification

The current results demonstrated that spectra combination improves determinations of selected odd and branched chain saturated (OBCFA) and *trans* unsaturated FA. For example, the best combinatorial model for the very minor (<0.50 g/100g of total fat) *iso* C17:0 FA was drastically improved and had the greatest decrease in RMSECV compared to all other FA (Fig. 2). The increase in robustness and simplicity of the latter was evident from the model's regression coefficients (RC) plot, which depicted variable combinations specific to *iso* C17:0 based on previously reported variables, specific for branched chain saturated FA standards, e.g. ATR/FTIR absorption in the vicinity of 1480–1430 cm^{-1} [17] and Raman scattering in the 2800–2700 cm^{-1} region [7] (Supporting materials, Fig. SM7). These RC were substantially smaller compared to the RC values of the ATR/FTIR variables in the vicinity of 1710 cm^{-1} and the Raman variables in the region of 3005 cm^{-1}, which emerged as the most important contributors (Supporting materials, Fig. SM7). It is possible that these two bands are correlated, as their loadings were aligned along the axis of principal component (PC) 4 in the two dimensional PC1–PC4 loadings plot (X-explained: 54%, 3%; Y-explained: 13%, 7%) of the *iso* C17:0 model. While the 1780–1700 cm^{-1} band is attributed to the C═O carbonyl absorption from the ester bond in the FA structure [18], no known molecular vibrations in saturated FA are assigned to the 3020–3000 cm^{-1} Raman region, which is rather better known as scattering from the symmetric and asymmetric stretching vibrations in =C–H ethylenic bonds of unsaturated FA, thus its significance in the determination of *iso* C17:0 was relatively unexpected [16]. Nevertheless, reports indicate that branched chain saturated FA standards exhibit similar Raman scattering when analyzed at FT conditions, but no explanation regarding the origin of the occurrence is provided [7]. The simplest unsaturated hydrocarbon ethylene $H_2C{=}CH_2$ has been shown to possess Raman spectrum with scattering signal in the vicinity of 3040 cm^{-1} from the asymmetric =C–H stretching vibration [23] and the length of this C–H bond in ethylene is 108.7 picometers (pm) [24]. Surprisingly, the simplest saturated alkane methane CH_4 also has a Raman scattering signal from the C–H stretching vibration around 3020 cm^{-1} [23,25], and the length of the C–H bond in methane (108.7 pm) is similar to ethylene's [26] (Supporting materials, Fig. SM8). However, in ethane the bond distance of the methyl C–H increases to 109.4 pm and in isobutane it is even longer reaching 111.3 pm [27] (Supporting materials, Fig. SM8). The Raman spectra of both ethane and isobutene do not exhibit such a scattering around the 3020–3000 cm^{-1} region at room temperature [28,29]. It would seem that the appearance of this band might be due to a shortened C–H chemical bond in the methyl end of the FA chain. As the molecules are cooled down, the aliphatic chains become more ordered by self-assembling. The existence of an extra $-CH_3$ group at the end of the FA chain, could induce strain conditions under which the organization of molecules becomes difficult and the *iso* branch is placed under stress due to proximity with other FA residues. This pressure could shorten the C–H bond and deform the electron cloud around C–H in $-CH_3$ from an isotropic to a highly dense distribution resembling that of =C–H, where the hydrogen atom is more closely attached to the carbon. Although shorter chemical bonds are associated with weaker polarizability, the electron cloud around the symmetrical vibration might be easily distorted upon interaction with the incident photons. A secondary technique (possibly X-ray diffraction) is required for obtaining the actual C–H bond length in the methyl group of FA during FT conditions for confirmation of this prediction. Nevertheless, as seen in the best *iso* C17:0 combinatorial model, as well as the appearance of the same region as significant in the *iso* C15:0 combinatorial model (although to a lesser extent, which could be due to lower *iso* C15:0 concentration (MAX=0.30 g/100 g in total fat, Table 1) and thus limited determination), the 3020–3000 cm^{-1} band is suspected to possess information about saturation under FT conditions.

The regression coefficients of the optimal C15:0 model using RFT Raman spectra combined with a no derivative pre-treated ATR/FTIR spectra indicated similar bands to previous reports (Supporting materials, Fig. SM2). One of the three significant predictors from the ATR/FTIR part of the spectra, the band around 1302 cm^{-1} related to $-(CH_2)_n-$ wagging vibrations was not previously observed in the single ATR/FTIR C15:0 models [17]. This very weak shoulder band is known to exhibit interaction with the proximate 1230 cm^{-1} band (Supporting materials, Fig. SM9), which is a strong band assigned to the C–O asymmetric stretching vibration in a C–O–C aliphatic ester bond (glycerol/hydrophilic part of TAG) [18]. Still, the appearance of this very weak band as a major contributor in the combinatorial, and not in the single model, might be driven by an interaction with the 1048 cm^{-1} band from the Raman spectrum. The loadings of all three bands were positioned along PC4 (0 angle, Y-explained: 30%, Supporting materials, Fig. SM10), which indicated that the angle between the loadings is small, which in turn means that these variables were correlated [30]. While the correlation between the 1300 cm^{-1} and 1230 cm^{-1} bands might be partially caused by proximity covariance, the nature of the 1300 cm^{-1} versus 1048 cm^{-1} interaction is solely due covariance present from different chemical bonds in the same molecule. Absorbance in the vicinity of 1305–1295 cm^{-1} is mass sensitive for *n*-alkanes and the Raman scattering in the region of 1100–1040 cm^{-1} is known to be due to the –C–C–C– stretching vibrations in the backbone of alkane residues [18]. The latter is the basis for interaction between these two FA chain length sensitive signals from two different spectroscopy techniques. It seems that the combinatorial model was able to pick up this interaction between the very weak ATR/FTIR band and the stronger Raman band in relation to C15:0 FA variations, which slightly improved linearity and decreased the residual error of the C15:0 model. Weak bands, which are normally not detected by variable selection algorithms, might emerge as significant when combined with other bands exhibiting similar vibrational modes.

Strong correlations between bands sensitive to similar vibrational modes were also evident in other fatty acid combinatorial models. For example, the covariance among the 976–956 cm^{-1} (ATR/FTIR) and the 1671–1665 cm^{-1} (Raman) bands in the total *trans* MUFA combinatorial models were due to the C═C bond in *trans* monounsaturated fatty acids. However, because these two signals are relatively isolated and strong in the individual ATR/FTIR and Raman spectra, this covariance seemed to result in a more accurate determination for the low total *trans* MUFA model only (Table 3, Fig. 4). Since most of the variation in relation to major fatty acids is directly available, weaker bands are deemed insignificant and typically removed by the variable selection algorithm. Nevertheless, the combinatorial approach seemed to enhance fatty acid specific signals and determinations for minor *trans* FA, such as *trans*-4 C18:1 were also enhanced (Supporting materials, Fig. SM11).

These results indicate that in addition to introducing extended variation, data combination might reveal band interactions from the two different types of spectra, which were previously not available. Covariance occurring due to vibrational signals from the same chemical bonds or signals from different bonds within the same molecule is evident. In turn, a higher abundance of FA

specific bands might help for the rejection of insignificant regions polluted with noise from similar or major FA and help for simplification of the prediction models.

Most new models result in an improved performance due to robustness and simplicity implied by the reduced number of model factors. The latter was especially evident in the OBCFA combinatorial model, which required only 2 PCs (Table 2) versus 6 PCs in the best single Raman prediction model [7] accompanied by fewer predictors (Supporting materials, Fig. SM12), as well as in the *trans*-11 C18:1 (only 1 PC) and total CLA (only 3 PCs) combinatorial models (Table 2). The lower number of PCs, which was accompanied by the lower amount of predictors necessary for description of the FA variation, is an important step towards a more robust identification of FA specific variables. If only a handful of the most important wavenumbers from different spectroscopy techniques are selected, construction of models based on multiple linear regression (MLR) might be possible. MLR is considered the most robust regression method for use in industrial at-line and on-line spectroscopy applications without the need for variable selection algorithms.

4.2. Variable selection strategies

A typical vibrational spectroscopy based chemometrical model does not always use the full range spectrum for the predictions, but often uses only a limited number of frequencies, which correspond (directly or indirectly) to the chemical structure of the predicted component. The selection procedures for these variables can differ, but the most commonly applied methodology involves the removal of the noisy/non-contributing variables (a backward elimination) by a selection algorithm, retaining only the important predictors (Scheme 2). The latter is typically performed in combination with the regression algorithm of choice and the regression method proven most robust in low observation, high predictor volume datasets, such as in spectroscopy based applications, is PLS regression.

The current results were highly dependent on the variable selection strategy. The backward variable elimination strategy starting from the fully concatenated ATR/FTIR and Raman spectra resulted in regression models with best overall performance. As previously indicated, the improvement in the performance of models constructed using this strategy was a result of new variable combinations from each Raman and ATR/FTIR spectrum. The forward variable input strategy, which only used variables selected in the single Raman models concatenated to full or selected ATR/FTIR regions, resulted in models with numerically better statistical parameters only for C17:0 and *trans*-5 C18:1 (Tables 2 and 3), while for all other FA a significant deterioration in R^2_{cv} and RMSECV performance was evident. In addition, most models using the forward strategy required more PCs, which denoted higher complexity. In contrast the backward variable selection strategy resulted in higher number of PCs only for the *trans*-4 C18:1 model, while for all others the number of PCs either remained the same or was drastically reduced compared to single spectra models (Table 3).

Although this higher model complexity in the forward variable selection approach might be driven by the incompatibility between the ATR/FTIR and the pre-selected Raman variables for describing the FA variation, no deterioration in the model's performance should have occurred and the jackknifing variable selection algorithm in combination with PLS should have been able to extract the original set of Raman only predictors for best performance. Nevertheless, it is possible that the selection algorithm was not capable of extracting this information, because it was overwhelmed by the high covariance between neighboring ATR/FTIR variables. Thus to achieve further "building" upon the best Raman only models, superior variable selection and/or regression methods should be investigated.

The advantage of the forward variable selection strategy is that it assumed that the best Raman only variables would always be the optimal solution, upon which new ATR/FTIR variables are added: similar to giving a 500 m head start in a 2 km track race. The drawback of this approach is that it undermines the combinatorial power of other variables, which might have emerged as significant in the original selection procedure. As it was subsequently discovered, it is these new variable combinations, which could give way to better sensitivity for description of the FA variation by helping in the detection of weak, but important vibrational modes.

4.3. Disadvantages of combinatorial spectroscopy

Combined Raman–ATR/FTIR spectra would allow the extraction of more chemical information regarding the sample of interest, but would impose the difficulties and the cost of having two separate spectroscopy systems. Although spectroscopy techniques are very fast (matter of seconds to few minutes, depending on the quality of spectra required), the new approach would also double the spectra acquisition time. Nevertheless, the industry has recognized this advantage and already there are instruments which combine two analytical techniques in a single system, but with separated compartments for sample analysis, e.g. Brüker Vertex 70 FTIR coupled to a RAM II Fourier transform Raman module (Bruker Analytical, Madison, WI). In addition, due to the significant advantages of possessing both Raman and IR spectral information, the development of combination instruments which generate spectra from the same sample portion (without moving the sample) with significant decrease in acquisition time are already underway, e.g. Horiba LabRAM IR^2 (HORIBA GmbH, Bensheim, Germany).

5. Conclusion

The new spectra combinatorial approach allows for addition of new fatty acid specific information to the regression models and allows for selection of weak fatty acid specific bands. This is achieved on the basis of "finding" covariance with other bands from the second type of spectra based on: (1) signal from the same bond, and (2) different bonds but within same molecule. In addition, the importance of variable selection algorithms in the construction and performance of chemometrics models is emphasized and a drawback of the jackknifing variable elimination algorithm in combination with PLS regression is exposed. For further optimization, new variable selection and regression opportunities, such as machine learning techniques should be explored.

A combination of spectra from two different techniques will provide fast solutions in various spectroscopy-based tasks, but the cost-benefit analysis should be seriously considered prior to application. From a speed point of view, obtaining spectra of a sample via a second vibrational spectroscopy technique would not disturb the routineness of the analysis. Thus this novel spectra combination approach should prove useful for a diverse range of applications in chemometrics, other than the currently demonstrated determination of milk fatty acids.

Acknowledgments

The Ph.D. research of Ivan Stefanov is supported by the Institute for the Promotion of Innovation by Science and Technology in Flanders (IWT), IWT-PhD-Project 60704.

Analyses on Raman spectroscopy as reported are obtained in collaboration with researchers of the Walloon Agricultural Research Centre, Valorisation of Agricultural Products Department (Head: Dr. Pierre Dardenne) within the framework of the collaborative agreement between LANUPRO and the Valorization of Agricultural Products Department (A08-TT-0384).

Appendix A. Supporting information

Supplementary data associated with this article can be found in the online version at http://dx.doi.org/10.1016/j.talanta.2013.02.034.

References

[1] Y. Ozaki, R. Cho, K. Ikegaya, S. Muraishi, K. Kawauchi, Appl. Spectrosc. 46 (1992) 1503–1507.
[2] V. Baeten, Lipid Technol. 22 (2010) 36–38.
[3] J. German, R. Gibson, R. Krauss, P. Nestel, B.T. Lamarche, W. van Staveren, J. Steijns, L. de Groot, A. Lock, F.D.R. Destaillats, Eur. J. Nutr. 48 (2009) 191–203.
[4] V. Fievez, E. Colman, J.M. Castro-Montoya, I. Stefanov, B. Vlaeminck, Anim. Feed Sci. Technol. 172 (2012) 51–65.
[5] R.G. Jensen, A.M. Ferris, C.J. Lammikeefe, J. Dairy Sci. 74 (1991) 3228–3243.
[6] H. Soyeurt, F. Dehareng, N. Gengler, S. McParland, E. Wall, D.P. Berry, M. Coffey, P. Dardenne, J. Dairy Sci. 94 (2011) 1657–1667.
[7] I. Stefanov, V. Baeten, O. Abbas, E. Colman, B. Vlaeminck, B. De Baets, V. Fievez, J. Agric. Food Chem. 58 (2010) 10804–10811.
[8] I. Stefanov, V. Baeten, O. Abbas, E. Colman, B. Vlaeminck, B. De Baets, V. Fievez, J. Agric. Food Chem. 59 (2011) 12771–12783.
[9] K. Scheerlinck, B. De Baets, I. Stefanov, V. Fievez, Comput. Electron. Agric. 73 (2010) 200–212.
[10] I. Stefanov, B. Vlaeminck, V. Fievez, J. Food Compos. Anal. 23 (2010) 852–855.
[11] P. Juaneda, M. Ledoux, J.L. Sebedio, Eur. J. Lipid Sci. Technol. 109 (2007) 901–917.
[12] S.A. Mjos, J. Chromatogr. A 1015 (2003) 151–161.
[13] J.K.G. Kramer, M. Hernandez, C. Cruz-Hernandez, J. Kraft, M.E.R. Dugan, Lipids 43 (2008) 259–273.
[14] C.A. Martin, C.C. de Oliveira, J.V. Visentainer, M. Matsushita, N.E. de Souza, J. Chromatogr. A 1194 (2008) 111–117.
[15] B. Vlaeminck, C. Dufour, A.M. van Vuuren, A.R.J. Cabrita, R.J. Dewhurst, D. Demeyer, V. Fievez, J. Dairy Sci. 88 (2005) 1031–1042.
[16] O. Abbas, J.A. Fernandez Pierna, R. Codony, C. von Holst, V. Baeten, J. Mol. Struct. 924 (26) (2009) 294–300.
[17] I. Stefanov, V. Baeten, O. Abbas, B. Vlaeminck, B. De Baets, V. Fievez, Evaluation of FT-NIR and ATR/FTIR spectroscopy techniques for determination of minor branched chain saturated and *trans* unsaturated fatty acids in milk fat, J. Agric. Food Chem. (2013) Article ASAP.
[18] G. Socrates, Infrared and Raman Characteristic Group Frequencies: Tables and Charts, Wiley, 2004.
[19] T. Davies, Something has happened to my data: potential problems with standard normal variate and multiplicative scatter correction spectral pretreatments, 2012, (accessed 7.1.10). Internet communication.
[20] J.E.D. Davies, J. Mol. Struct. 31 (1976) 217–231.
[21] J.G. Grasselli, Croat. Chem. Acta 61 (1988) 745–761.
[22] K.S. Kalasinsky, Trac-Trends Anal. Chem. 9 (1990) 83–89.
[23] J.F. Verdieck, S.H. Peterson, C.M. Savage, P.D. Maker, Chem. Phys. Lett. 7 (1970) 219–222.
[24] M.J.S. Dewar, H.N. Schmeising, Tetrahedron 11 (1960) 96–120.
[25] S.B. Hansen, R.W. Berg, E.H. Stenby, Appl. Spectrosc. 55 (2001) 745–749.
[26] J.F. Stanton, Mol. Phys. 97 (1999) 841–845.
[27] R.L. Hilderbr, J.D. Wieser, J. Mol. Struct. 15 (1973) 27–36.
[28] K. Van Helvoort, W. Knippers, R. Fantoni, S. Stolte, Chem. Phys. 111 (1987) 445–465.
[29] J.C. Evans, H.J. Bernstein, Can. J. Chem.-Rev. Can. Chim. 34 (1956) 1037–1045.
[30] The Unscrambler™ Camo A/S, A multivariate statistical analysis program, 2008. Internet communication.